

ANALYSIS OF FACIES AND FRACTURES WITH RESPECT TO
PRODUCTION IN THE BAKKEN FORMATION,
PARSHALL/SANISH FIELDS, WILLISTON
BASIN, NORTH DAKOTA

by
Matthew Billingsley

A thesis submitted to the Faculty and the Board of Trustees of the Colorado School of Mines in partial fulfillment of the requirements for the degree of Master of Science (Geology).

Golden, Colorado
Date 11/3/11

Signed: Matthew Billingsley
Matthew Billingsley

Signed: Stephen A. Sonnenberg
Dr. Stephen A. Sonnenberg
Thesis Advisor

Signed: Thomas L. Davis
Dr. Thomas L. Davis
Thesis Advisor

Golden, Colorado
Date 11/3/11

Signed: John Humphrey
Dr. John Humphrey
Professor and Head
Department of Geology and Geological Engineering

ABSTRACT

The Bakken Formation has recently become an important petroleum reservoir in the Williston Basin, despite containing relatively poor reservoir characteristics. Parshall/Sanish Fields lie east and updip of the main Bakken depocenter, where large amounts of oil were generated in thermally mature, organic-rich upper and lower Bakken shales. The Bakken Formation is an Upper Devonian-Lower Mississippian carbonaceous shale and dolomitic siltstone to fine-grained sandstone with low average porosity (3 to 5 percent) and permeability (0.01-0.05md). The low matrix permeability of this reservoir increases the importance of other types of reservoir properties, such as natural fractures.

Natural fractures can develop at numerous scales and in response to a variety of mechanisms, such as tectonics and hydrocarbon generation. The focus of this study is to: 1) examine the main causes of natural fractures, 2) determine the relationship of fractures to the various facies present within the middle Bakken reservoir, and 3) understand the impact of fractures on oil production.

The study area is roughly 900 square miles, and encompasses the highly productive Parshall/Sanish fields, as well as less to non-productive areas to the east. This study used: 1) detailed analysis on 12 cores to identify facies of the middle Bakken Formation; 2) identification of quantity and type of natural fractures in each facies to determine the relationship of fractures to facies; 3) optical mineralogy to understand the role of mineralogy on the creation of microfractures.

The middle member can be divided into six main facies based on lithology, grain size, sedimentary structures, and trace fossils. Fractures were observed in the cores and correlated to the various facies of the middle Bakken member. Microfractures were also observed in petrographic thin sections and the highest density of microfractures occurs in dolomite-rich, laminated intervals. The quantity of fractures identi-

fied within the cores does not show a correlation to the highest producing wells within the study area.

TABLE OF CONTENTS

ABSTRACT	iii
LIST OF FIGURES	viii
ACKNOWLEDGEMENTS	xiv
CHAPTER 1 INTRODUCTION	1
1.1 Location of Study Area	2
1.2 Research Objectives and Methods	2
1.3 Previous Work	3
CHAPTER 2 GEOLOGICAL OVERVIEW	13
2.1 Sedimentology and Stratigraphy of the Williston Basin	13
2.2 Regional Structure	17
2.3 Petroleum Geology	18
2.4 The Bakken Petroleum System	20
2.5 The Hydrocarbon Trap at Parshall/Sanish	22
2.6 Production History	27
CHAPTER 3 FACIES IDENTIFICATION, CORE DESCRIPTIONS, AND FA- CIES DISTRIBUTION	31
3.1 Methodology and Background	31
3.2 Facies Descriptions	34
3.2.1 Facies A - Skeletal Lime Wackestone	34
3.2.2 Facies B - Bioturbated, Argillaceous Siltstone	36
3.2.3 Facies C - Planar to Wavy Laminated Calcareous Siltstone	38

3.2.4	Facies D - Massive to Low-Angle Cross-Stratified Very Fine to Fine-Grained Sandstone	41
3.2.5	Facies E - Wavy to Ripple Laminated Dolomitic Siltstone	42
3.2.6	Facies F - Muddy, Dolomitic Siltstone	44
3.3	Core Descriptions	44
3.3.1	Braaflat #11-11H (Sec. 11-T153N-R91W)	47
3.3.2	Fertile #1-12H (Sec. 12-T151N-R90W)	48
3.3.3	Jensen #12-44 (Sec. 12-T154N-R90W)	50
3.3.4	Long #1-01H (Sec. 1-T152N-R90W)	52
3.3.5	MHA #1-18H (Sec. 18-T150N-R90W)	54
3.3.6	N & D #1-05H (Sec. 5-T152N-R90W)	56
3.3.7	Parshall #2-36H (Sec. 36-T153N-R90W)	59
3.3.8	Patten #1-27H (Sec. 27-T153N-R89W)	59
3.3.9	Rogstad #1-11 (Sec. 11-T155N-R91W)	61
3.3.10	Sikes State #44-16H (Sec. 16-T154N-R91W)	63
3.3.11	St Andes #151-89-2413H-1 (Sec. 24-T151N-R89W))	65
3.3.12	Van Hook #1-13H (Sec. 13-T152N-R91W)	68
3.4	Facies Distribution	68
3.5	The Origin and Role Dolomite in the Middle Bakken	76
3.5.1	Mixing-Zone Dolomitization Model	82
3.5.2	Evaporative-Sabkha or Seepage Reflux Dolomitization Model	82
3.5.3	Seawater Dolomitization Model	82
3.5.4	Burial Dolomitization	84

3.5.5 Dolomite Discussion	84
CHAPTER 4 FRACTURE AND WELL LOG ANALYSIS	87
4.1 Experimental Fractures	87
4.2 Natural Fractures	88
4.2.1 Regional Fractures	88
4.2.2 Tectonic Fractures	89
4.2.3 Hydrocarbon-generated Fractures	91
4.2.4 Fractures Associated with Laminated Siltstones and Shales	93
4.3 Fracture Analysis in Core	93
4.3.1 Types of Fractures in Core	94
4.3.2 Fractures Analysis Conclusions	95
4.3.3 Well Log Analysis with Associated Fractures	97
4.4 Microfractures	111
4.5 Fractures vs. Production	112
CHAPTER 5 CONCLUSIONS AND RECOMMENDATIONS	127
5.1 Recommendations	128
REFERENCES CITED	131

LIST OF FIGURES

Figure 1.1	Map showing the south limit of the Bakken Formation (dashed line) and the location of the study area in northwestern North Dakota. Modified from Meissner (1978).	2
Figure 1.2	Net pay map (in feet) for the middle Bakken member determined from water saturation values equal to or less than 40%. From Simenson (2009).	10
Figure 1.3	Hydrocarbon pore volume map of the middle Bakken member showing the increase in hydrocarbons in the middle of Parshall/Sanish Fields. The map was created by multiplying a grid of the net thickness of the middle Bakken by the grid of average porosity by the grid of average oil saturation (1-Sw). From Simenson (2009).	11
Figure 2.1	Generalized stratigraphic column of the Williston Basin with sequences that represents major transgressive-regressive events and some of the major producing formations (*). From Gerhard et al. (1987).	14
Figure 2.2	Map showing the lateral extent of the Williston Basin and some of the major structural features. Modified from Gerhard et al. (1982).	18
Figure 2.3	Structure map of the top of the middle Bakken showing the low angle WSW dip. The hydrogen index (HI) contour lines indicate increased maturity (lower HI values) of the upper and lower Bakken shale members toward the main Bakken depocenter. HI data from Price et al. (1984).	21
Figure 2.4	Generalized stratigraphic column of the Upper Devonian-Lower Mississippian formations that make-up the Bakken petroleum system. Modified from Webster (1984).	23
Figure 2.5	Paleogeographic map showing the location of the Williston Basin during Late Devonian time (365 Ma), which corresponds to the beginning of Bakken deposition. Modified from Blakey (2011).	24
Figure 2.6	Oil, water, and gas production chart for Parshall/Sanish Fields. Modified from North Dakota Geological Survey.	28
Figure 2.7	Upper Bakken structure map with estimated ultimate recovery (EUR) of Bakken wells within Parshall and Sanish Fields.	30

Figure 3.1	Comparison of several author's facies models for the middle Bakken member. From CSM Bakken Consortium (2010).	32
Figure 3.2	Location map of the 12 cores used in the approximately 900 square-mile study area. The large and small boxes are the townships and ranges, respectively.	33
Figure 3.3	Facies descriptions of the six middle Bakken Facies: A, B, C, D, E, and F with associated core photographs. CSM Bakken Consortium (2010).	35
Figure 3.4	Contact (black line) between the lower Bakken shale (LBS) and the overlying Facies A of the middle Bakken for the Braaflat #11-11H well.	37
Figure 3.5	Core photo of the heavily bioturbated Facies B from the Braaflat #11-11 core. Note the presence of pyrite nodules (P).	39
Figure 3.6	Core photo of the wavy laminated Facies C from the Braaflat #11-11 core. Note the thin mud drapes separating the silty layers, which suggests tidal deposition and the wavy nature of the laminations, which may represent microbial influence at the time of deposition.	40
Figure 3.7	Core photo of the high energy sandstone, Facies D, from the Braaflat #11-11 core.	43
Figure 3.8	Core photo of the wavy to ripple laminated dolomitic siltstone, Facies E from the Braaflat #11-11 core. Note the wavy laminations and the zone of bioturbation indicative of Facies E.	45
Figure 3.9	Core photo of Facies F from the Braaflat #11-11 core. Note the presence of brachiopod shells (B), which are prevalent within this facies.	46
Figure 3.10	Core descriptions for the Braaflat #11-11 well.	49
Figure 3.11	Core descriptions for the Fertile #1-12H well.	51
Figure 3.12	Core descriptions for the Jensen #12-44 well.	53
Figure 3.13	Core descriptions for the Long #1-01H well.	55
Figure 3.14	Core descriptions for the MHA #1-18H well.	57
Figure 3.15	Core descriptions for the N & D #1-05H well.	58

Figure 3.16 Core descriptions for the Parshall #2-36H well.	60
Figure 3.17 Core descriptions for the Patten #1-27H well.	62
Figure 3.18 Core descriptions for the Rogstad #1-11 well.	64
Figure 3.19 Core descriptions for the Sikes State #44-16 well.	66
Figure 3.20 Core descriptions for the St. Andes #151-89-2413H-1 well.	67
Figure 3.21 Core descriptions for the Van Hook #1-13H well.	69
Figure 3.22 Facies to log correlation with associated core photos for the six middle Bakken Facies using GR, Rt, RHOB, NPHI, and DPHI logs. Note the clean GR and high Rt of the Facies D sandstone and the GR marker at the base of Facies E.	70
Figure 3.23 Map showing the core locations used for the various stratigraphic cross-sections (A-A', B-B', and C-C').	71
Figure 3.24 N-S stratigraphic cross-section of the middle Bakken facies A, B, C, D, E, and F. Note the thinning of the middle Bakken to the south and the intermittent presence of Facies D.	73
Figure 3.25 NW-SE stratigraphic cross-section through Parshall Field, showing the thinning of the middle Bakken to the SE and the intermittent presence of Facies D.	74
Figure 3.26 N-SE stratigraphic through Parshall Field showing the lack of Facies C and D throughout much of Parshall Field.	75
Figure 3.27 Isopach map of Facies A and B of the middle Bakken member. Facies A and B thin to the east, and average 15 to 25 ft within Parshall/Sanish fields.	77
Figure 3.28 Isopach map of Facies C of the middle Bakken member. Facies C thins and pinches out to the east, within Parshall Field. The thinning of Facies C may serve as a stratigraphic trap within Parshall Field.	78
Figure 3.29 Isopach map of Facies D of the middle Bakken member. Facies D is largely absent in Parshall Field, but occurs in thick intervals within Sanish Field.	79

Figure 3.30	Isopach map of Facies E and F of the middle Bakken member. These facies thicken to the northeast, and average 10 ft within Parshall/Sanish fields.	80
Figure 3.31	Isopach map of the upper Bakken member. The upper Bakken member averages 17 ft within Parshall/Sanish Fields.	81
Figure 3.32	Models for early dolomitization, induced by relative changes in sea-level. From Purser et al. (1994).	83
Figure 4.1	Map showing the orientation of the maximum shear stress and the direction of natural fractures oriented parallel to the Sh Max of N55°E. Data from NDIC files, oriented Mission Canyon cores at Little Knife (Narr and Burruss, 1984), and regional maximum horizontal stress directions from (Whiting, 2010) and (Zoback and Zoback, 1980).	90
Figure 4.2	Photos of the four main types of fractures observed and recorded in the core samples: A) vertical fracture, B) Hairline associated with a microfault, C) Calcite cemented fracture, and D) Open horizontal fracture.	96
Figure 4.3	Fracture counts associated with each facies and associated well log characteristics for the Braaflat 11-11H well. The Braaflat 11-11H core averages 1.2 fractures/ft.	100
Figure 4.4	Fracture counts associated with each facies and associated well log characteristics for the Fertile 1-12H well. The Fertile 1-12H core averages 2 fractures/ft.	101
Figure 4.5	Fracture counts associated with each facies and associated well log characteristics for the Long 1-01H well. The Long 1-01H core averages 5.1 fractures/ft.	102
Figure 4.6	Fracture counts associated with each facies and associated well log characteristics for the MHA 1-18H well. The MHA 1-18H core averages 1 fracture/ft.	103
Figure 4.7	Fracture counts associated with each facies and associated well log characteristics for the N & D 1-05H well. The N & D 1-05H core averages 4.2 fractures/ft.	104
Figure 4.8	Fracture counts associated with each facies and associated well log characteristics for the Parshall 2-36H well. The Parshall 2-36H core averages 2.1 fractures/ft.	105

Figure 4.9	Fracture counts associated with each facies and associated well log characteristics for the Patten 1-27H well. The Patten 1-27H core averages 8.6 fractures/ft.	106
Figure 4.10	Fracture counts associated with each facies and associated well log characteristics for the Rogstad 1-11 well. The Rogstad 1-11 core averages 5.4 fractures/ft.	107
Figure 4.11	Fracture counts associated with each facies and associated well log characteristics for the Sikes State 44-16 well. The Sikes State 44-16 core averages 0.4 fractures/ft.	108
Figure 4.12	Fracture counts associated with each facies and associated well log characteristics for the St Andes 151-89 well. The St Andes 151-89 core averages 3.4 fractures/ft.	109
Figure 4.13	Fracture counts associated with each facies and associated well log characteristics for the Van Hook 1-13H well. The Van Hook 1-13H core averages 3.8 fractures/ft.	110
Figure 4.14	Qemscan mineralogy for the Deadwood Canyon Ranch #43-28H well, located in Sanish Field. Note the increase in dolomite toward the top of the middle Bakken (Facies E and F). Modified from Simenson (2009).	112
Figure 4.15	Core photograph of Facies E (9279 ft) in the Parshall #2-36 well. The associated thin section photo is located below in Figure 4.16. Core photo from the NDIC.	113
Figure 4.16	Thin section photograph showing a natural, pyrite-filled horizontal microfracture within Facies E. The fracture is located at the boundary between the dolomitic, quartz-rich layer and the dark brown, clay-rich layers.	114
Figure 4.17	Core photo of Facies E (9281 ft) in the Parshall #2-36 well. The associated thin section photo is located below in Figure 4.18. Core photo from the NDIC.	115
Figure 4.18	Thin section photograph showing the presence of both open and pyrite-filled microfractures within Facies E. The well-rounded to sub-rounded white grains are silt-sized quartz and the dark brown matrix between the grains is clay. The dark black color between the grains and within the fracture is pyrite; blue is porosity. Note the fractures following the boundary between the quartz-rich layers and the dark brown, clay-rich layers.	116

Figure 4.19	Core photograph of Facies E (9282 ft) in the Parshall #2-36 well. The associated thin section photo is located below in Figure 4.20. Core photo from the NDIC.	117
Figure 4.20	Thin section photograph of Facies E, identifying the presence of a possible bitumen-filled fracture. The large white grains are silt-sized quartz (Q) and the smaller euhedral grains are dolomite (D).	118
Figure 4.21	Core photograph of Facies F (9276 ft) in the Parshall #2-36 well. The associated thin section photo is located below in Figure 4.22. Core photo from the NDIC.	119
Figure 4.22	Thin section photograph of Facies F, identifying the presence of open fractures. The blue color of the fractures indicates porosity. Note the presence of echinoderm spine shells (SP) and other shell fragments in the upper half of the photograph.	120
Figure 4.23	Core photograph of the upper Bakken shale (9272 ft) in the Parshall #2-36 well. The associated thin section photo is located below in Figure 4.24. Core photo from the NDIC.	121
Figure 4.24	Thin section photograph of the upper Bakken shale, identifying the presence of open, natural horizontal microfractures.	122
Figure 4.25	Production bubble map of maximum monthly oil production for the Bakken cores used in the study with associated fractures. The top number is maximum monthly oil production (bbls) and the bottom number is the amount of fractures/ft.	124
Figure 4.26	Map showing the location and orientation of the horizontal wells within Parshall/Sanish Fields. Note the more east-west orientation and longer lateral lengths in Sanish Field.	125

ACKNOWLEDGEMENTS

I would like to give a special thanks to numerous people for their continued support throughout graduate school. First, I would like to thank Tom Davis for finding and funding this project through the Colorado School of Mines Reservoir Characterization Project (RCP). It was truly a pleasure and honor to work with Tom and be a member of RCP. I definitely increased my knowledge of all things geophysical in nature. RCP also provided the opportunity to hone my presentation skill, whether it was in front of the RCP students and professors or in front of over 200 RCP sponsors from all over the world. Special thanks to Tom for continuing to support the Lone Ranger throughout this entire process. I would also like to thank all of the RCP students, sponsors, and Bob Benson for their support, knowledge, and intellectual discussions. I would also like to specifically thank Newfield Exploration for their financial support and for allowing me the opportunity to do an internship while working on my thesis project.

I would also like to thank Steve Sonnenberg for supporting me from the first day that I arrived at Mines. I truly appreciate all of the discussions, whether related to the Bakken or not, that we had in your office before everyone else arrived on campus. I also want to thank Steve for allowing me the opportunity to be involved in the Bakken Consortium, where I quickly gained knowledge of the Bakken during our bi-weekly Bakken meetings. Thank you to all of the Bakken Consortium members and sponsors for your thought provoking discussions related to the Bakken. I would also like to thank Rick Sarg and John Curtis for agreeing to be on my committee and for providing continued discussion and support.

Lastly, but certainly not least, I would like to thank my parents, Lee and Joanne, for their continued love and support throughout my life. I cannot imagine two more supportive parents. I would also like to specifically thank my father for his willingness

and desire to discuss my thesis with him at any time of day. Your support and inspiration is definitely the main reason that I have been able to get through this entire process, which will hopefully lead to following in your footsteps in becoming a successful petroleum geologist.

CHAPTER 1

INTRODUCTION

The Bakken Formation has become an important petroleum reservoir in the Williston Basin of North Dakota and Montana, despite containing relatively poor reservoir characteristics. Parshall/Sanish fields, two of the most productive fields in the entire Williston Basin, lie east and updip of the main Bakken depocenter, where large amounts of oil were generated in thermally mature, organic-rich upper and lower Bakken shales. The extremely low matrix permeability (0.0001-.01 mD) of this reservoir increases the importance of other types of reservoir-enhancing properties, such as the presence of natural fractures.

The Bakken Formation is a relatively thin unit of Upper Devonian-Lower Mississippian-aged, organic-rich shale and dolomitic siltstone located within the deeper parts of the Williston Basin, United States. The Bakken Formation is generally divided into three main members: 1) organic-rich black shale (lower member), 2) silty dolostone to fine-grained sandstone (middle member), and 3) organic-rich black shale (upper member). The upper and lower shale members are organic-rich source rocks that expelled oil into low-porosity and low-permeability reservoirs such as the middle Bakken member and underlying Three Forks Formation.

Parshall and Sanish Fields are located within Mountrail County, North Dakota, approximately 90 miles east of the Montana border. Parshall Field was discovered in 2006, with the EOG Parshall 1-36 discovery well that had an initial production rate of 463 BOPD. The main target of the field is the Bakken Formation, specifically targeting the low porosity, low permeability middle Bakken reservoir. Since 2006, EOG and several other operators have increased horizontal drilling operations, making Parshall and Sanish Fields two of the most productive fields in the Williston Basin. As of January 2011, both Parshall Field and Sanish Field have an average monthly

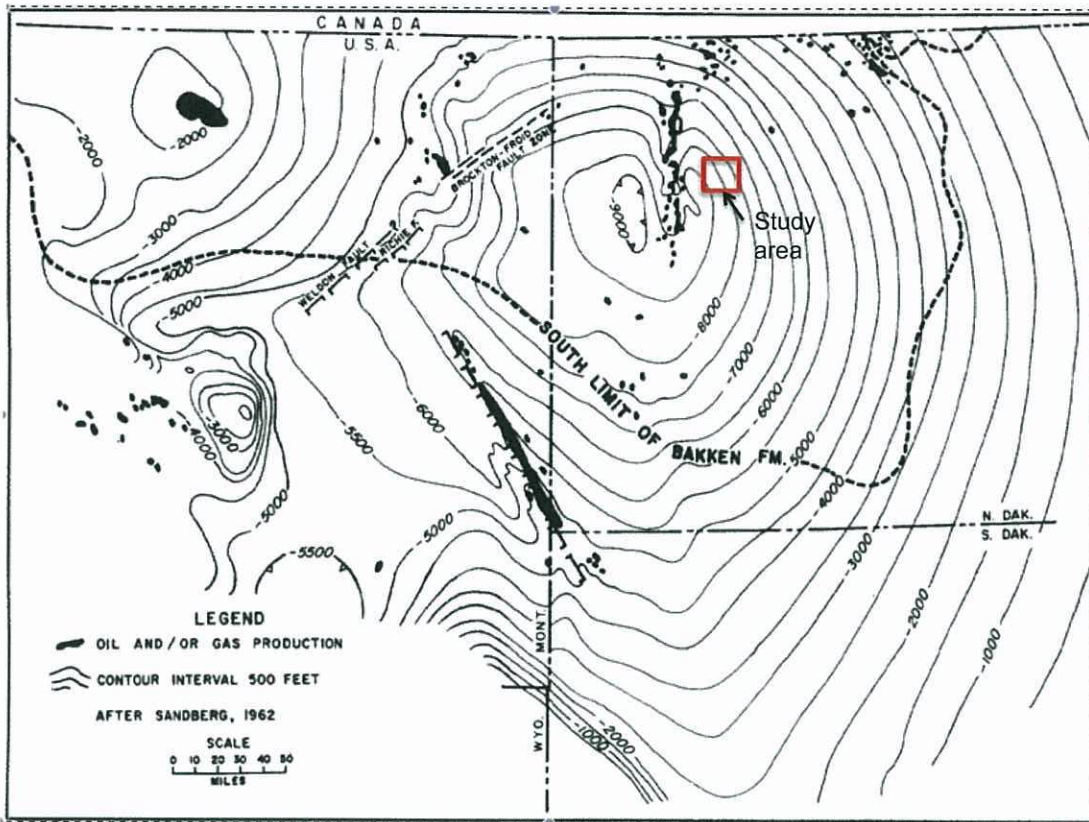


Figure 1.1: Map showing the south limit of the Bakken Formation (dashed line) and the location of the study area in northwestern North Dakota. Modified from Meissner (1978).

production of approximately 1 million barrels of oil per month.

1.1 Location of Study Area

The study area is a roughly 900 square mile area located in Mountrail County, North Dakota. Specifically, the study area covers Townships 150N-155N and Ranges 86W-91W (Figure 1.1).

1.2 Research Objectives and Methods

Parshall/Sanish Fields contain some of the highest initial oil production rates in the Williston Basin, despite the extremely low matrix permeability of the middle

Bakken reservoir. The main Bakken depocenter lies west of Parshall/Sanish Fields, where the organic shales of the upper and lower Bakken are buried in the deepest, most mature part of the basin. The upper and lower Bakken shales located in Parshall/Sanish Fields are less mature than their downdip counterparts to the west. The enormous oil accumulations discovered in Parshall/Sanish Fields, despite being located in between less mature shales, strongly suggest that oil has migrated updip from the depocenter and become trapped in Parshall/Sanish Fields. The extremely low matrix permeability of the middle Bakken Formation also suggests that other porosity and permeability enhancing mechanisms, such as natural fractures, are present to allow for oil migration.

The purpose of this study is to determine the: 1) cause of natural fractures in the Bakken; 2) relationship of fractures to facies; 3) impact of fractures on oil production. This study discusses natural fractures associated with regional stress fields, local tectonics, overpressuring, and hydrocarbon generation. The study involves observing fractures in both core and petrographic thin sections to determine if certain facies within the middle Bakken are more susceptible to fracturing. The next step was to understand the main reasons for increased fracture susceptibility within each facies by observing variations in clay content, presence of laminations, proximity to mature shales, variations in mineralogy, etc. If certain facies can be identified and related to fracturing, then mapping of these facies may lead to better identification of fracture networks.

1.3 Previous Work

Fred Meissner published a classic paper in 1978 titled "Petroleum Geology of the Bakken Formation Williston Basin, North Dakota and Montana." Meissner (1978) discusses a variety of geologic and petroleum aspects of the Williston Basin, but perhaps none more important than the presence and effect of source rock maturity and

overpressuring in the Bakken Formation in Antelope field, McKenzie County, North Dakota. He plotted electrical resistivity versus depth to identify the depth of hydrocarbon generation. He concluded that high-resistivity occurs at subsea depths of -6200 to -8200 ft, which represents the zone of mature source rocks and thus hydrocarbon generation. He also illustrated how the pressure gradient changed from 0.46 psi/ft in the overlying Lodgepole Formation to 0.73 psi/ft. in the Bakken Formation, and then shifts back to 0.47 in the underlying Nisku Formation.

Meissner (1978) further illustrated the direct relationship between abnormally high fluid pressure and hydrocarbon generation associated with mature source rocks. He stated that anomalous pressures in the Bakken are believed to be maintained by the combination of large hydrocarbon volumes generated at high rates and the relative isolation of the Bakken by extremely tight rocks in the underlying Three Forks and overlying Lodgepole Formations. He then described the importance of fluid overpressuring and differential stress to create open tension fractures that create reservoir conditions.

James W. Schmoker and Timothy C. Hester wrote a paper in 1983 titled "Organic Carbon in Bakken Formation, United States Portion of Williston Basin." Schmoker and Hester (1983) compared calculated organic-carbon values to 59 laboratory organic-carbon analyses of Bakken shales from 39 wells in North Dakota, with organic-carbon contents ranging from 6 to 20%. A plot of the organic-carbon content calculated in laboratory experiments was compared to log-derived formation density. This relation indicated a negative correlation, where an increase in the log-derived density corresponds to lower total organic carbon (TOC). This negative correlation leads to the premise that the density-log in the upper and lower Bakken shales varies primarily in response to changes in organic matter. A positive correlation exists between the TOC values determined from core analysis and the TOC values determined from the density log. This provides a proxy for determining the TOC values using the density

log only, when no core analysis is available.

Schmoker and Hester (1983) also calculated average total organic carbon (TOC) values for 159 locations in North Dakota and 107 locations in Montana. Their results indicate average TOC values of 12.1% for the upper Bakken member and 11.5% for the lower Bakken member, which are considerably higher than the suggested minimum threshold for a source-rock of 2-2.5% (J.C. Curtis, pers. comm.). These average TOC values are in close agreement with the 13% average previously determined by Webster (1982), but are drastically higher than the average of 3.8% reported by (Williams, 1974).

In 1982, Lee C. Gerhard et al. published a paper titled "Geological Development, Origin, and Energy Mineral Resources of Williston Basin, North Dakota." Gerhard et al. (1982) focused on the sedimentology, stratigraphy, and structure of the Williston Basin. They used the Sloss (1963) sequence concept to breakout the stratigraphy of the Williston Basin into six major sequences based on major transgressive cycles. The authors are in agreement with Carlson (1960) and Carroll (1979) that basement blocks that were structurally defined in the Precambrian control both the sedimentation and structure of the basin. The authors described how the main seaway connection to the basin changed throughout time due to various episodes of uplift, subsidence, and sea-level fluctuations.

Structural movement of the Nesson anticline initiated in the Precambrian, as evidence by Lower Deadwood sediments being deposited around, but not over, the crystalline core of the anticline. Abrupt changes in thickness across the structure indicate fault movement along the west flank of the Nesson anticline. A mid-Permian event changed the stress regime and changed the motion of the fault to up on the west from down on the west. Later Laramide-related strain is evident during the pre-Late Cretaceous by reversal of movement along the Nesson fault. Since then, there has been little evidence of major fault movement (Gerhard et al., 1982).

The authors state that the Williston Basin has subsided approximately 16,000 ft since Middle Ordovician time without undergoing severe orogenic deformation. The authors mention that mapping of heat gradients by Harris et al. (1981) suggests no presence of abnormally high heat flow that would indicate mantle plume or hot spots beneath the basin to account for this subsidence. They also mention that several papers were written about advanced wrench-fault systems to account for the generation of structural elements in the Williston Basin, but that none have championed a specific origin for the Williston Basin. The authors hypothesize that the Fromberg and the Colorado-Wyoming shear zones were formed by left-lateral shearing on the edge of the Precambrian continental plate, which displaced the present northern and southern Rocky Mountain blocks.

Leigh Price et al. wrote a paper in 1984 titled "Organic Metamorphism in the Mississippian-Devonian Bakken Shale North Dakota Portion of the Williston Basin." The main focus of this paper was on the organic geochemistry of Bakken oils as they relate to maturity. The authors explain the suppression of R_o values in the Bakken when compared to Tertiary through Middle Jurassic sediments. This is due to the change in organic matter from oxygen-rich, terrestrially-derived organic matter to a marine-derived organic matter. The authors used this knowledge to conclude that much higher burial temperatures were required for both the threshold of intense hydrocarbon generation and mainstage hydrocarbon generation.

Julie LeFever has conducted extensive studies in the North Dakota portion of the Williston Basin and has written numerous papers concerning the Bakken Formation. For Example, LeFever et al. (1991), conducts detailed lithofacies descriptions on the middle Bakken members. LeFever et al. (1991) identifies and describes seven lithofacies for the middle Bakken members. Canter et al. (2009) also describes facies and subfacies of the middle Bakken in Mountrail County, North Dakota. The facies descriptions between LeFever et al. (1991) and Canter et al. (2009) are similar, with the